




A spontaneous missense mutation in the chromodomain helicase DNA-binding protein 8 (*CHD8*) gene: a novel association with congenital myasthenic syndrome

C. Y. Lee*†, M. Petkova*† , S. Morales-Gonzalez*†, N. Gimber‡, J. Schmoranzer‡, A. Meisel§, W. Böhmerle§, W. Stenzel¶ , M. Schuelke*†  and J. M. Schwarz*†

*NeuroCure Cluster of Excellence, †Department of Neuropediatrics, ‡Advanced Medical Bioimaging Core Facility (AMBIO), §Department of Neurology and ¶Department of Neuropathology, Charité–Universitätsmedizin Berlin, Corporate Member of Freie Universität Berlin, Humboldt-Universität zu Berlin, and Berlin Institute of Health, Berlin, Germany

C. Y. Lee, M. Petkova, S. Morales-Gonzalez, N. Gimber, J. Schmoranzer, A. Meisel, W. Böhmerle, W. Stenzel, M. Schuelke and J. M. Schwarz (2020) *Neuropathology and Applied Neurobiology* 46, 588–601

A spontaneous missense mutation in the chromodomain helicase DNA-binding protein 8 (*CHD8*) gene: a novel association with congenital myasthenic syndrome

Aims: Congenital myasthenic syndromes (CMS) are characterized by muscle weakness, ptosis and episodic apnoea. Mutations affect integral protein components of the neuromuscular junction (NMJ). Here we searched for the genetic basis of CMS in female monozygotic twins. **Methods:** We employed whole-exome sequencing for mutation detection and Sanger sequencing for segregation analysis. Immunohistology was done with antibodies against CHD8, rapsyn, β -catenin (β CAT) and golgin on fibroblasts, human and mouse muscle. We recorded superresolution images of the NMJ using 3D-structured illumination microscopy. **Results:** We discovered a spontaneous missense mutation in *CHD8* [chr14:g.21,884,051G>A, GRCh37.p11 | c.1732C>T, NM_00117062 | p.(R578C)], the gene encoding chromodomain helicase DNA-binding protein 8. This is the first missense mutation affecting Duplin, the short 110 kDa isoform of

CHD8. It is known that CHD8/Duplin negatively regulates β CAT signalling in the WNT pathway and plays a role in chromatin remodelling. Inactivating *CHD8* mutations are associated with autism spectrum disorder and intellectual disability in combination with facial dysmorphism, overgrowth and macrocephalus. No muscle-specific phenotype has been reported to date. Co-immunostaining with rapsyn on human and mouse muscle revealed a strong presence of CHD8 at the NMJ being located towards the sarcoplasmic side of the rapsyn cluster, where it co-localizes with β CAT. **Conclusion:** We hypothesize CHD8 to have a role in the maintenance of the structural integrity and function of the NMJ. Both patients benefited from treatment with 3,4-diaminopyridine, a reversible blocker of voltage-gated potassium channels at the nerve terminal that prolongs the action potential and increases acetylcholine release.

Keywords: Duplin, myasthenia, overgrowth, macrocephalus, neuromuscular junction, superresolution microscopy

Correspondence: Jana M. Schwarz, Department of Neuropediatrics, Charité Universitätsmedizin Berlin, D-13353 Berlin, Germany. Tel: +49 (0)30 450 539038; Fax: +49 (0)30 450 539965; E-mail: jana-marie.schwarz@charite.de

Markus Schuelke, Department of Neuropediatrics, Charité Universitätsmedizin Berlin, D-13353 Berlin, Germany. Tel: +49 (0)30 450 566112; Fax: +49 (0)30 450 66920; E-mail: markus.schuelke@charite.de

Introduction

Congenital myasthenic syndromes (CMS) are a heterogeneous group of mostly autosomal-recessive disorders affecting the structural integrity of the neuromuscular junction (NMJ). Clinical features comprise muscle hypotonia, increased muscle fatigability, ptosis and episodes of apnoea. Further characteristics are muscle weakness, especially of the ocular, bulbar and proximal limb muscles. The disease manifests early, often perinatally or during early childhood. Several genes are known to be implicated in CMS. Most of them encode essential structural components of the NMJ such as (i) subunits of the presynaptic proteins involved in neurotransmitter release and recycling, (ii) proteins of the synaptic basal lamina and (iii) proteins of the postsynaptic acetylcholine receptor (AChR) clusters [1]. The CMS can be subclassified into presynaptic, synaptic and postsynaptic forms, as well as into ubiquitous forms caused by deficient glycosylation of NMJ components. Myasthenic symptoms may also be caused by antibodies against proteins of the NMJ through transplacental acquisition in transient myasthenia of the neonate or through autonomous production in *myasthenia gravis* [2]. The diagnostic workup of patients with suspected CMS involves, beyond genetic testing, clinical examination, electromyography and the search for antibodies against AChR or the muscle-specific kinase (MuSK). CMS therapy is aimed to control the symptoms by improving neuromuscular transmission.

Here, we report 14-year-old monozygotic twins with myasthenia-like symptoms in whom we found a spontaneous heterozygous missense mutation in *CHD8*. This gene encodes the Chromosomal helicase domain protein 8 which, due to alternative splicing exists in two long 290 kDa (NM_001170629) and 262 kDa (NM_020920) [3], and several shorter isoforms; among them a C-terminally truncated isoform without the helicase domain, a protein called Duplin (for axis duplication inhibitor) [3,4]. CHD8 belongs to the CHD family of ATP-dependent chromatin remodelling enzymes that are responsible for regulation of DNA accessibility and thus for gene expression [5]. CHD8 is implicated in transcriptional regulation of the canonical WNT pathway [3,5-7]. Depending on the cellular receptor repertoire, WNT signalling can be categorized as canonical or noncanonical and is implicated in cell proliferation,

morphology, motility, axis formation and organ development [8]. In canonical WNT signalling, extracellular WNT proteins bind to the membrane receptor frizzled, activate dishevelled, which in turn inhibits β -catenin (β CAT) phosphorylation by glycogen synthase kinase 3 β (GSK3 β). Phosphorylated β CAT is degraded by the proteasome, whereas WNT mediated inhibition of phosphorylation stabilizes β CAT, allowing it to accumulate in the nucleus and stimulate transcription of WNT target genes [9]. In muscle cells, canonical WNT signalling reduces the expression of rapsyn, a protein that anchors and clusters the AChR in the postsynaptic membrane, thus being essential for the postsynaptic maturation of the NMJ [10,11]. In complex with transcription factor 4 (TCF4), β CAT serves as a transcriptional coactivator [12]. CHD8/Duplin was initially discovered as a direct interaction partner and negative regulator of β CAT [3,6,13]. CHD8 inhibits the binding of β CAT to TCF4, thereby repressing the transcription of WNT3a- and β CAT-dependent genes [5,6]. The influence of CHD8 on WNT target genes seems to be tissue dependent with negative regulation in non-neuronal cells (e.g. muscle) and positive regulation in neuronal progenitor cells [14].

Case history

All patients provided written informed consent according to the Declaration of Helsinki for all aspects of the study and for publication of the facial photographs.

The now 14-year-old female monozygotic twins are the first children of healthy nonconsanguineous German parents. Pre-eclampsia required Caesarean section at 31 + 6 weeks of gestation. Neonatal complications comprised respiratory distress, cardiorespiratory instability, jaundice, ptosis and muscle weakness. Macrocephalus with an occipito-frontal head circumference of 33 cm (z-score = 2.91) was already present at birth. Head control and motor development were delayed with free ambulation achieved at 2.5 years of age. Walking improved at first but deteriorated later at 6 years with frequent falls and generally increased muscle fatigability. At 11 years of age, both girls developed a rapidly progressive scoliosis, which was treated with a corset. The parents reported frequent gastrointestinal problems with constipation starting in early infancy.

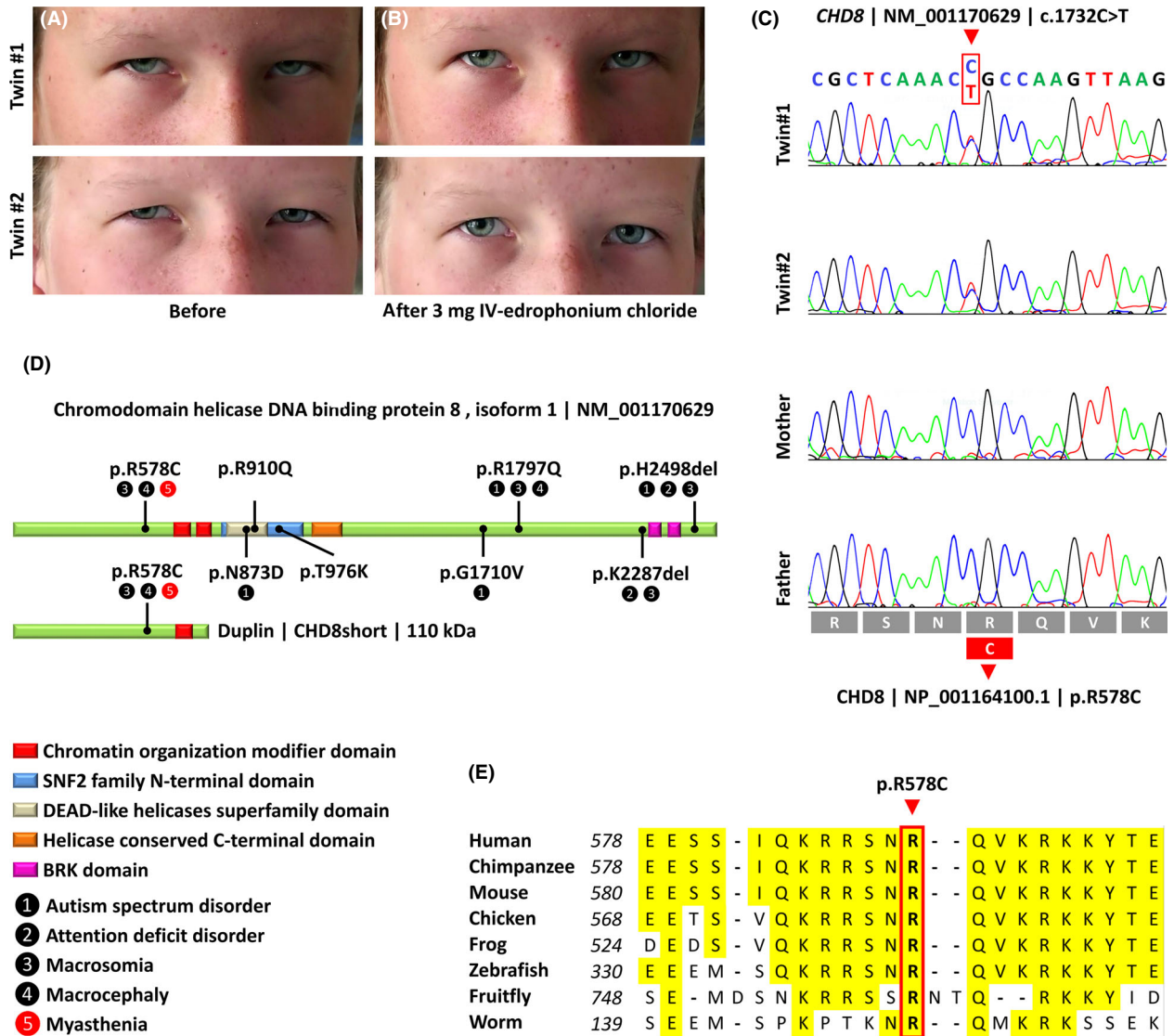


Figure 1. Ptosis in both twins (A) before and (B) 1 min after fractionated IV injection of 3 mg edrophonium chloride. Besides reduction of ptosis, the patients reported self-perceived improvement of eye opening and manual force. The effect only lasted some minutes. (C) Sanger sequencing electropherograms of the spontaneous *CHD8* missense mutation [chr14:g.21,884,051G>A, GRCh37.p11], which was only present in the twins, but absent in both parents. (D) Linear depiction of the protein-domain structure of the long (290 kDa) and the short (110 kDa) isoform (Duplin). The p.R578C mutation affects both isoforms. Locations of the other published missense mutations are marked as well. The numbers highlight crucial phenotypical characteristics of the patients. The various protein domains are marked by colour and are drawn to scale. (E) Multispecies alignment of CDH8 homologs. The mutant amino acid and its sequence context are conserved down to *Caenorhabditis elegans*. Accession numbers: Human, NP_001164100.1; Chimpanzee, ENSPTRG00000006124; Mouse, ENSMUSG00000053754; Chicken, XP_025001761; Frog, XP_018115294.1; Zebrafish, ENSDARG00000075543; Fruitfly, XP_016022893.1; Worm, XP_003090036.1. [Colour figure can be viewed at wileyonlinelibrary.com]

At the age of 11.6 years, the body height of both girls was 165.5/170 cm (z-score = 1.94/2.54) and the head circumference 60.5 cm (z-score = 4.82). Further symptoms comprised bilateral ptosis, hypomimia, hypertelorism, down-slanting palpebral fissures (Figure 1A) and a weak voice. Eye movements were normal without diplopia. Muscle reflexes were normal, but muscle force

in the legs was reduced to Medical Research Council (MRC) scores 3-4 out of 5 [15], tending to worsen after exertion or in cold weather. Both girls have a thoracolumbar scoliosis, valgus knee deformities and planus feet. They have a waddling gait with inverted forefeet. Repetitive electric stimulation of the median nerve did not show a decrement in the adductor pollicis brevis

muscle action potential amplitudes. Muscle biopsy specimens were not available for analysis. Motor and sensory nerve conduction velocities were normal. The intravenous edrophonium chloride test was positive (Figure 1A,B) with a short and also self-perceived improvement, of eye opening and grip force. We excluded in both patients the presence of auto-antibodies against PQ-type voltage-gated calcium-channel, AChR, MuSK and Titin as known causes of or being associated with myasthenic syndromes. For differential diagnosis of the overgrowth, we investigated bone age and hormone status (IGF1, IGF1-BP3, fT4, TSH), which were all normal, as were the results of cMRI, echocardiography, ECG and chromosome analysis.

Both girls attend the seventh grade of a normal school with average performance. Intelligence was assessed with the Kaufman Assessment Battery for Children II and yielded average results for both girls in the scales Sequential/Gsm (short-term memory) and Simultaneous/Gv (visual processing). Results for Learning/Glr (long-term retrieval) and Planning/Gf (fluid reasoning) were slightly below average. Both girls are well integrated at school and do not have difficulties of social communication/interaction or establishing eye contact and do not show restricted or repetitive behaviour, which excludes an autism spectrum disorder (ASD).

We initiated pyridostigmine treatment (8 mg/kg BW/day) with only minor improvement of the gait pattern. Salbutamol (0.04 mg/kg BW/day) was added after 6 weeks, but both drugs had to be discontinued due to severe gastrointestinal symptoms and vertigo. A clear and persistent improvement of gait pattern, muscle weakness and fatigability was only achieved with 3,4-diaminopyridine (3,4-DAP; 0.5 mg/kg BW/day for the past 14 months), which enabled the patients to walk for more than 1 h, climbing stairs, carrying and lifting shopping bags. 3,4-DAP is a reversible blocker of voltage-gated potassium channels at the nerve terminal, which increases the duration of the action potential allowing a greater ACh release. Under 3,4-DAP therapy, a single-fibre electromyography (EMG) yielded normal results (Figure S1).

Materials and methods

Whole-exome sequencing

DNA was isolated from peripheral leucocytes. Whole-exome sequencing (WES) was done only in one twin,

after monozygosity had been established by multiple microsatellite marker analysis. Exonic sequences and flanking intronic regions were captured using the SureSelect® human all exon V5 kit (Agilent Technologies, Santa Clara, California, USA) and sequenced on an Illumina HiSeq 4000 machine yielding 53.4 Mio paired-end FASTQ reads. These were aligned to the human GRCh37.p11 genomic reference with BWA-MEM v0.7.1 [16]. 99.1% of the SureSelect® V5 positions were covered >10×, and 97.8% >20×. After fine-adjustment, the raw alignments were called for deviations from the reference sequence in all coding exons and 50 bp flanking regions using GATK v3.8 [17]. The resulting VCF file was analysed with MutationTaster2 [18] to assess potential pathogenicity of all variants. For the recessive inheritance model, we removed variants that occurred >10× in homozygous state in the ExAC database (homozygote frequency >1.7E-04) and looked for homozygous or compound heterozygous mutations. For the dominant inheritance model, we removed variants that occurred >10× in heterozygous state in the ExAC database (MAF >8.3E-05).

Potentially disease-causing variants were further assessed for their pathogenicity using the additional information provided by MutationTaster2 at <http://www.mutationtaster.org> (accessed April 2019) and visually inspected using the IGV software downloaded from <http://www.broadinstitute.org/igv/>. Relevant variants were tested for segregation in the family by automatic Sanger sequencing using the BigDye® Terminator v3.1 chemistry (Applied Biosystems, Waltham, Massachusetts, USA) on the ABI 3500 Genetic Analyzer. For verification of the CHD8 variant (Figure 1C) and for segregation testing, we used the oligonucleotide primers FW 5'-TTC ATG AAA ATT TTG GAG TAG AAT C-3', REV 3'-GGA ATC TCT CGA GCC TCG GA-5'. We additionally tested a variant in SH2B1 [chr16:g.28,880,618A>T, CRCh37p.11 | c.215A>T ENST00000538342] using the oligonucleotide primers FW 5'-TTC ATG AAA ATT TTG GAG TAG AAT C-3' and REV 3'-CAT TCG ACA TTT GAG TTT ACT AAA GT-5'.

Immunohistology

CHD8/golgin co-immunostaining of patient and control fibroblasts: Patient and control fibroblasts were cultured in DMEM supplemented with 15% foetal calf serum to

semiconfluency, fixed with 4% buffered paraformaldehyde, permeabilized with 0.1% Triton X-100 and quenched with 0.1 M glycine and blocked with 10% goat serum. The fibroblasts were labelled with primary antibodies against CHD8 (ab114126; Abcam, Cambridge, UK, 1:50 dilution, the antibody recognizes amino acids 604–629 of human CHD8, NP_001164100.1) and against golgin (sc-73619, 1:100 dilution; Santa Cruz Biotechnology, Dallas, Texas, USA) at 4°C overnight and subsequently with appropriate secondary fluorescently labelled antibodies (AlexaFluor488, AlexaFluor568). Nuclei were labelled with DAPI (Vector Laboratories, Burlingame, California, USA). Images were recorded by epifluorescence and confocal imaging using a Leica DMI 4000B inverted microscope and a CARVII (Becton Dickinson, Franklin Lakes, New Jersey, USA) spinning disk scan head.

CHD8/rapsyn/ β CAT co-immunostaining of control muscle sections and on isolated muscle fibres. Muscles and single-muscle fibres were derived from *Dmd*^{EGFP} mice [19], which express dystrophin-EGFP fusion protein from the endogenous locus. Therefore, GFP staining corresponds to/detects dystrophin. Single-muscle fibres were prepared according to Pasut *et al.* [20]. *Quadriceps* muscle cryosections or single-muscle fibres isolated from *extensor digitorum longus* muscles were fixed with 4% or 2% buffered paraformaldehyde, respectively, incubated in preheated 0.01 M citric acid pH 6.0 for 15 min at 80°C for antigen retrieval, and permeabilized with 0.1% Triton X-100. The muscle section/fibres were then quenched with 0.1 M glycine, blocked with 5% normal goat serum, and labelled with primary antibodies against GFP (A01694, 1:250; GenScript Biotech, Piscataway, New Jersey, USA), CHD8 and rapsyn (sc-58585, 1:30 dilution; Santa Cruz) or β CAT (610153, 1:30 dilution; BD) at 4°C overnight and subsequently with appropriate secondary fluorescently labelled antibodies (AlexaFluor—488, —568, —647). Nuclei were labelled with DAPI. Samples were mounted in ProlongGlass Antifade Mountant (ThermoFisher Scientific, Waltham, Massachusetts, USA).

3D structured illumination microscopy

3D three colour structured illumination microscopy (SIM) images were acquired using the 488, 568 and 642 nm laser lines, standard filter settings and 125 nm z-sectioning of the OMX V4 Blaze (GE

Healthcare, Chicago, Illinois, USA) system. 100 nm fluorescent beads (Tetraspeck, T7284, Thermo Fischer Scientific) were used for registration of the detection channels, achieving <40 nm registration error for all three channels. 3D-rendering, image- and movie export was done with Arivis Vision4D and ImageJ [21].

Results

Mutation screening

In the WES data set we discovered a novel variant in *CHD8* [chr14:21,884,051G>A, GRCh37.p11 | c.1732C>T, NM_001170629 | p.(R578C)] exchanging an evolutionary highly conserved arginine for a cysteine in the glutamine-rich domain of CHD8. As the parents were unrelated, we applied two different filter models, one assuming dominant inheritance and one assuming recessive inheritance. The recessive model revealed only a single variant in *SLAIN1* affecting an exon that is not transcribed in most transcripts. The dominant model yielded 10 candidate variants that caused an amino acid change and had a low allele frequency in the gnomAD database (Table S2). Two variants, one in *CHD8* and one in *SH2B1*, were shortlisted due to the cellular functions of these genes, a loss of which might serve as explanation for our patients' phenotype. The *SH2B1* variant was excluded because it was present in the healthy father. The *CHD8* variant was absent in both parents and we opted for this spontaneous mutation as the most likely disease gene candidate. The *CHD8* variant fulfils the PS2, PM2 and PP3 criteria of the American College of Medical Genetics and Genomics [22] placing it in the 'likely pathogenic' category.

Immunohistology

Immunofluorescent staining of fibroblasts from patients and controls showed a diffuse cytoplasmic distribution of CHD8 with clear enrichment around the Golgi apparatus, which was verified by co-immunostaining with anti-CHD8 and antigolgin antibodies. We did not find any difference in the subcellular distribution of CHD8 in fibroblasts between patients and controls (Figure S2).

Due to the myasthenic symptoms of our patients, we investigated single-isolated mouse muscle fibres (Figure 2), as well as cryosections from murine (Figure 2) and human muscle (Figure S3) for the presence of

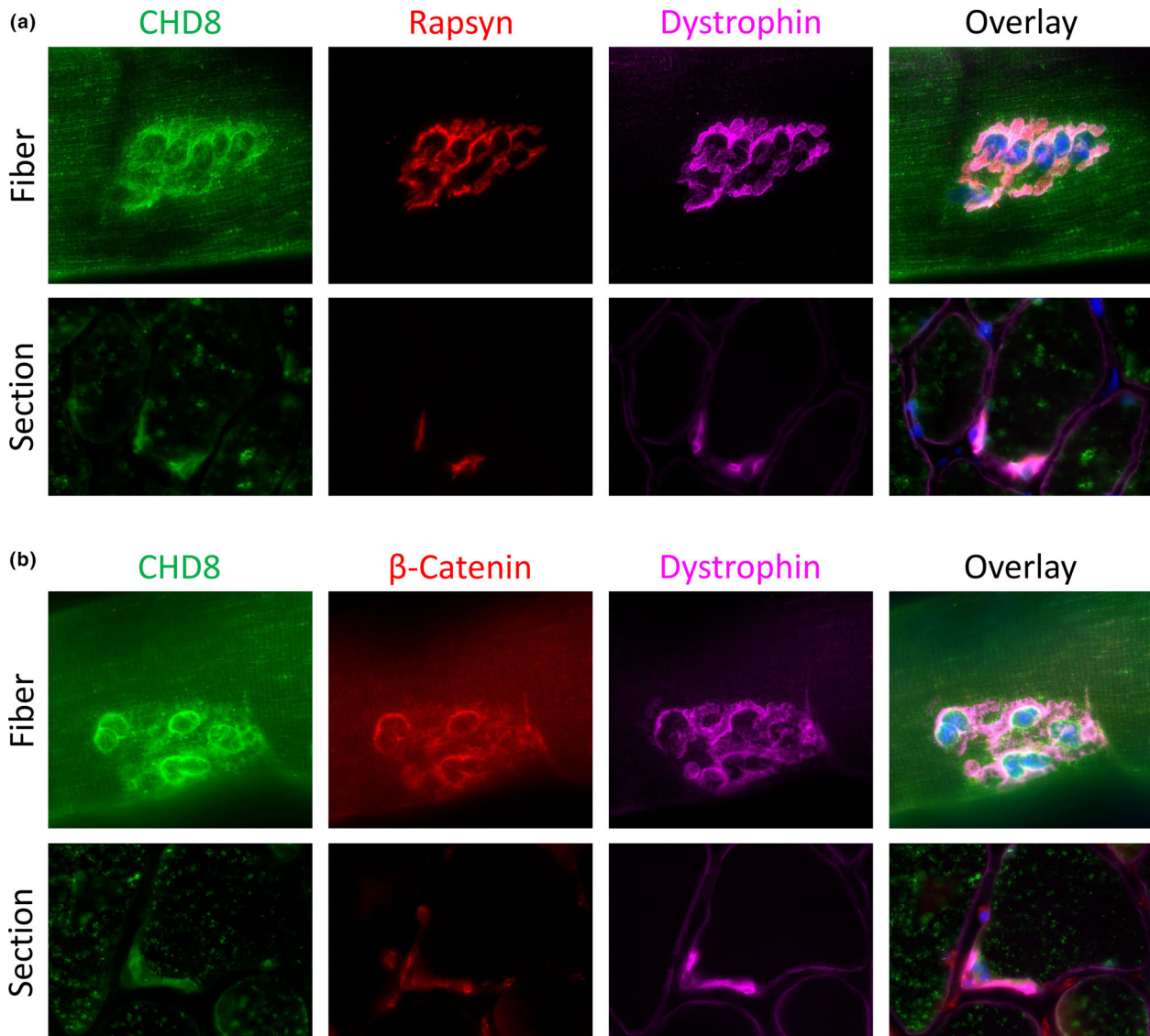


Figure 2. (A) CHD8/rapsyn/dystrophin and (B) CHD8/ β -catenin (β CAT)/dystrophin co-immunostaining of isolated murine *EDL* muscle fibres and of *quadriceps* muscle cross sections. (A,B) The green CHD8/Duplin signal was scattered throughout the sarcoplasm, but highly enriched at the neuromuscular junction (NMJ), which is marked by the red rapsyn signal. The anti-CHD8-antibody recognizes AA 604-629 at the vicinity of the mutation in the N-terminal domain of CHD8/Duplin. The dystrophin signal (magenta) delineates the sarcoplasmic membrane and is also enriched at the NMJ. (B) β CAT co-localizes with CHD8/Duplin at the NMJ. Beyond that, the here employed anti- β CAT antibody recognizes β CAT located in the nuclei (B, lower panel). Nuclei are stained with DAPI and are blue on the overlays. [Colour figure can be viewed at wileyonlinelibrary.com]

CHD8, especially in the vicinity of the NMJ that was marked with antirapsyn antibodies. A muscle biopsy of the patients was unfortunately not available for investigation. In healthy muscle fibres, CHD8 was diffusely distributed in the sarcoplasm with high enrichment in the subsarcolemmal region. Superresolution 3D-SIM confirmed a strong CHD8-signal at the NMJ, and provided a better resolution in the z-plane; the CHD8-

signals were located below the rapsyn layer where they could be visualized in close proximity to the β CAT signals (Figure 3; Video S1; Figure S5).

Discussion

We describe a dominant spontaneous mutation in *CHD8* in identical twins who presented with

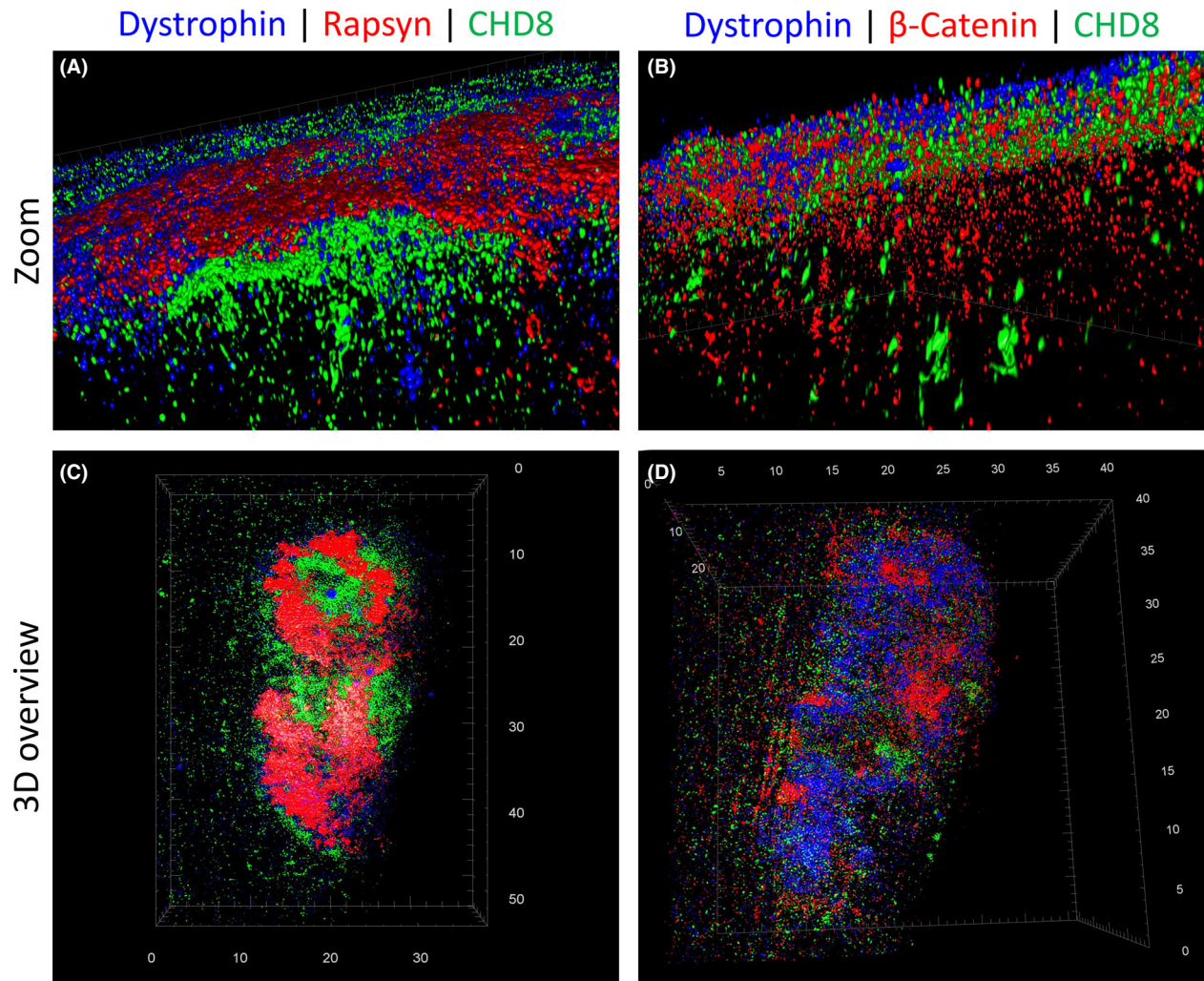


Figure 3. 3D structured illumination microscopy of the neuromuscular junction (NMJ) in isolated murine muscle fibres. Superresolution images were taken after triple-immunostaining with the same protocols as for Figure 2. The 3D rendered z-stacks are depicted in panels A,C [CHD8/rapsyn/dystrophin] and B,D [CHD8/ β -catenin (β CAT)/dystrophin]. The boundary box displays the scale in micrometres (μ m). The single channels of the decomposed images A,B are depicted on Figure S5. The nonrendered maximum intensity z-projections of C,D are depicted on Figure S4. To get a better rendition of the 3D structure from all sides, we provide Videos S1 and S2. (A) The zoom into the NMJ clearly demonstrates the CHD8 layer (green) to be located beneath the rapsyn layer (red) towards the sarcoplasm. Dystrophin is depicted in blue. (B) β CAT (red) and CHD8/Duplin (green) are in close proximity in the same layer beneath the sarcoplasmic membrane, as highlighted by dystrophin (blue). We did not detect any presynaptic CHD8/Duplin. [Colour figure can be viewed at wileyonlinelibrary.com]

myasthenia, muscle weakness, ptosis, macrocephalus and overgrowth. Myasthenia has to date not been reported in association with *CHD8* mutations. The clinical phenotype of patients with *CHD8* mutations does vary, but macrosomia, macrocephalus, ASD [14,23,24] and gastrointestinal problems [25-37] appear to be constant features [29,38]. Some reports mention muscle hypotonia, however, in cases of microdeletions it often remains unclear, whether a certain symptom might be caused by *CHD8* deficiency *per se* or by

derangement of neighbouring genes [25]. The majority of disease-associated variants are *de novo* microdeletions [25,33,38] and frameshift mutations [29,35,38]. So far, only one other missense mutation (p.R1797Q) and two deletions of one amino acid (p.K2287del; p.H2498del) have been published along with phenotype descriptions [29]. Four more mildly affected patients with missense mutations (p.N873D, p.R910Q, p.T976K, p.G1710V) have been published, however, without detailed phenotype description [29,39]. The

location of these alterations and the corresponding phenotypes are depicted on Figure 1D and in Table S1. The following muscle symptoms were mentioned in four individuals out of 66 patients with *CHD8* mutations (Raphael Bernier, personal communication): muscle hypotonia ($n = 2$), abnormal muscle tone ($n = 1$), reduced muscle strength in the arms ($n = 1$). The location of the p.R578C variant at the N-terminus of the protein is of special interest as this mutation is the only one that affects both the short Duplin isoform as well as the full-length isoforms (Figure 1D). Mutations associated with ASD are mostly inactivating mutations that affect the helicase domain, which is known to play a role in chromatin remodelling. The short Duplin isoform still contains the nuclear localization signal and the β CAT-binding site, making it an active inhibitor of the WNT signalling pathway [4]. The anti-CHD8 antibody we used in this study does recognize both Duplin and the long isoforms.

For the following reasons, we think the c.1732C>T *CHD8* variant to be disease causing: (i) the variant occurred spontaneously and is absent in the gnomAD database, (ii) the mutant codon (CGC>TGC, p.Arg578) is highly conserved on the DNA-level with a PhyloP score of 5.2 (range -14 to $+6$) and a PhastCons score of 1 (range 0 to 1) [40,41] as well as on the amino acid level in vertebrates. The exchange of an arginine for a cysteine replaces a positively charged side chain with one with a thiol-group marked by a high Grantham score of 180 (range 0 to 215) [42]. While the mutation does not cause subcellular mislocalization of CHD8 as shown by immunohistology of patient and control fibroblasts (Figure S2), protein folding and interaction with binding partners might be affected, (iii) our patients' phenotype with macrocephalus and overgrowth overlaps with key features of previously published patients with *CHD8* mutations from the ASD spectrum. (iv) We have excluded mutations in other genes (Supporting Information) that might be responsible for a CMS or overgrowth phenotype. Analysis of the panel of $n = 35$ genes associated with CMS only yielded one heterozygous variant in *AGRN*, analysis of the 'overgrowth panel' yielded none. According to the Standards and Guidelines for the Interpretation of Sequence Variants developed by the *American College of Medical Genetics and Genomics*, the c.1732C>T variant can be classified as a 'likely pathogenic' sequence variation, because it occurred spontaneously in the patients

and was absent in the parents (PS2), and in controls from the gnomAD database (PM2), the affected gene is known to cause a large part of the phenotype if mutated (PP4), and computational evidence supports a deleterious effect of the mutation on the gene (PP3) [22].

Mutations affecting *CHD8* are strongly associated with ASD and macrocephalus. ASD was notably absent in our patients and their cognitive abilities were within the normal range. This was surprising as ASD and intellectual disability were considered defining key features to be associated with *CHD8* mutations.

The presence of ptosis and other myasthenic symptoms in our patients broadens the phenotypic spectrum and highlights CHD8 or its short isoform Duplin as a protein relevant for muscle function, especially at the NMJ. Due to its manifold functions in gene expression and regulation of WNT signalling, we hypothesize CHD8/Duplin to have a dual role at the NMJ by (i) regulating expression of NMJ-relevant genes and by (ii) being involved in its structural integrity. During NMJ formation the presence of densely clustered AChRs in the postsynaptic membrane is a basic requirement [43,44]. This clustering is highly controlled by various pre and postsynaptic factors. In the developing myotome, binding of WNT to the muscle-specific tyrosine kinase (MuSK) and the lipoprotein receptor-related-protein 4 (LRP4) at the postsynaptic membrane initiates formation of AChR microclusters [45-47] at the centre of the muscle fibre, to where axons are guided. The neuron-derived signalling molecule agrin then binds to postsynaptic LRP4 and MuSK facilitating the formation of fully sized AChR clusters of the mature muscle [48-51]. These clusters are anchored in the membrane by the protein rapsyn [52]. On the sarcoplasmic side, rapsyn interacts with β CAT to connect the complex via β CAT with the cytoskeleton [53]. This interaction is highly dynamic with respect to removal or insertion of new AChRs [54]. Muscle-derived WNT3a signals through frizzled 8 and β CAT/GSK3 β , thereby reducing rapsyn expression. This directly opposes agrin-mediated AChR clustering [10]. A fine balance of AChR clustering dynamics seems to be pivotal for synaptic integrity (Figure 4).

CHD8 is ubiquitously expressed with higher levels in brain and neuronal tissue (Human Protein Atlas) [55,56]. However, the effects of mutations may be tissue-specific due to interaction with other tissue-specific

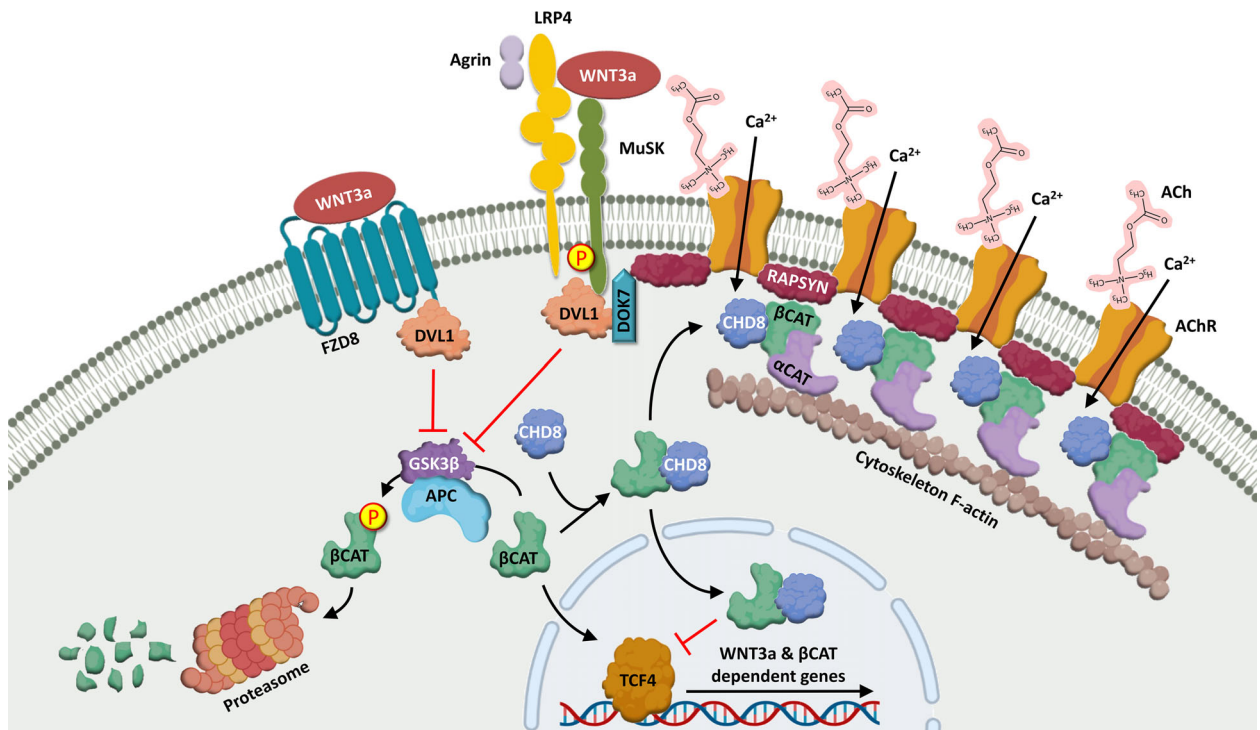


Figure 4. Illustration of the canonical WNT- and LRP4/MuSK mediated pathways at the postsynaptic side of the neuromuscular junction. β -catenin (β CAT) accumulates in the cytoplasm and is phosphorylated and subsequently degraded by the proteasome. Binding of WNT3a to frizzled 8 (FZD8) during canonical WNT signalling, activates dishevelled (DVL1), which in turn inhibits β CAT phosphorylation by the glycogen synthase kinase 3 β /APC-WNT signalling pathway regulator complex (GSK3 β :APC). β CAT is then free to translocate into the nucleus, where it acts as transcriptional co-activator for transcription factor 4 (TCF4) in the transcription of WNT-dependent genes. Binding of agrin and WNT3a to the muscle-specific tyrosine kinase (MuSK) and the lipoprotein receptor related-protein 4 (LRP4) activates DVL1 and docking protein 7 (DOK7) which facilitates AChR clustering *via* rapsyn. Rapsyn connects the AChRs *via* β CAT and β CAT to the F-actin filaments of the cytoskeleton. Expression of chromodomain helicase DNA-binding protein 8 (CHD8) in the cytosol and its binding to β CAT would (i) reduce canonical WNT signalling to the nucleus and (ii) increase the CHD8/ β CAT building blocks for the AChR clusters. [Colour figure can be viewed at wileyonlinelibrary.com]

proteins. CHD8 insufficiency alters the expression of many genes as demonstrated by RNA-sequencing following siRNA-mediated knockdown in human neural progenitor cells [57]. Among them were also genes relevant for the NMJ such as *CHRNA4*, *CHRNA7*, as well as *LRP4*. *CHRNA4*, *CHRNA7* encode the β 4- and β 7-subunits of the nicotinic AChR. Mutations of *LRP4* are associated with CMS type 17 (MIM #616304). A further gene that is differentially expressed upon *CHD8* knockdown is *NRG1*, encoding for neuregulin 1. Neuregulin 1 modifies AChR clustering at the NMJ *via* its interaction with MuSK. At the same time, it activates local gene transcription [58] leading to an increase in mRNA-copies for *CHRNE*. This gene encodes the β -subunit of the AChR that replaces the β -subunit (*CHRNA7*) of the AChR during development

[59]. Mice with a heterozygous *Nrg1* deletion had myasthenic symptoms and the amount of mRNA coding for AChR subunits was decreased [60].

We hypothesize that the myasthenia-like symptoms of our patients could be explained by a muscle-specific function of CHD8/Duplin (Figure 4) either as (i) transcriptional regulator or as (ii) structural component of the NMJ (Figures 2 and 3): CHD8/Duplin directly interacts with β CAT in an inhibitory manner to down-regulate the expression of β CAT target genes in the WNT pathway [3]. However, β CAT does not only function as a transcription co-activator. In muscle cells, it serves as a structural component of the NMJ. Through interaction with rapsyn it links the AChRs to the cytoskeleton *via* β CAT (Figure 4) [53]. Muscles from β CAT knockout mice showed enlarged NMJ areas, widely distributed

AChR clusters, and motoneuron mislocation. Interestingly, these mice did not only exhibit postsynaptic alterations, but their presynaptic ACh neurotransmitter release was disturbed, indicating defects in vesicle fusion or exocytosis from the presynaptic nerve terminal. The authors postulated that β CAT may play a role in the presynaptic muscle differentiation through retrograde signalling [61]. These results would nicely fit with our observation that 3,4-diaminopyridine, a pharmacological substance allowing a larger ACh release from the presynaptic nerve terminal would be beneficial in our patients.

Experiments in myotubes of *Rapsn*^{-/-} mice have shown that rapsyn was indispensable for the β CAT induced AChR clustering [62]. This interaction is further enforced by agrin [62], which in turn is dependent on β CAT to induce AChR aggregation [53]. Our results from immunohistological co-localization studies showed that CHD8 and rapsyn are located side-by-side, which might suggest a role for CHD8/Duplin in AChR receptor clustering as well, probably through direct interaction with rapsyn-bound β CAT. The missense mutation in our patients might impede such specific interactions. In this regard, CHD8/Duplin may serve as a modulator during NMJ formation by (i) nudging the system towards clustering of AChRs by increased synthesis of rapsyn (through alteration of the WNT/ β CAT mediated transcription) and by (ii) providing CHD8/ β CAT building blocks for consolidation of the AChR clusters. However, more research is required into the interactions and dynamics of CHD8 expression at the NMJ.

In conclusion, we describe a heterozygous spontaneous mutation in *CHD8*, which we assume to cause the myasthenia-like phenotype in association with macrocephalus and overgrowth. However, more patients with N-terminal CHD8/Duplin mutations have to be found in order to delineate a specific genotype–phenotype relation. The myasthenic symptoms of our patients broaden the phenotypic spectrum of *CHD8* mutations and suggest a role of CHD8/Duplin in NMJ maintenance and function. Further molecular and electrophysiological experiments should be conducted to specify the muscular function of CHD8/Duplin. Patients with *CHD8* mutations should be specifically investigated for neuromuscular symptoms and *CHD8* should be included into CMS panel diagnostics.

Acknowledgements

We thank the patients and their family for participation in this study. This research was funded by grants of the Deutsche Forschungsgemeinschaft (DFG; German Research Foundation) under Germany's Excellence Strategy – EXC-2049-390688087 to MS, and to JMS by the Nachwuchs kommission of the Charité Berlin (Rahel-Hirsch scholarship). NG was supported by a grant of the Deutsche Forschungsgemeinschaft (SFB958/Z02) to JS.

Ethical approval

The study was approved by the local ethical review board of the Charité (EA1/228/08).

Conflict of interest

None declared. The Editors of *Neuropathology and Applied Neurobiology* are committed to peer-review integrity and upholding the highest standards of review. As such, this article was peer-reviewed by independent, anonymous expert referees and the authors (including WS) had no role in either the editorial decision or the handling of the paper.

Author contributions

Chae Young Lee: analysed the genetic data, recorded microscopic images, wrote the first draft of the manuscript together with JMS; Mina Petkova: performed the immunohistological staining in the mouse; Niclas Gimber, Mina Petkova and Jan Schmoranzler: performed the superresolution SIM recordings; Susanne Morales-Gonzalez: performed immunohistological stainings and microscopy in human muscle and fibroblasts; Andreas Meisel: phenotyped and referred the patients; Wolfgang Böhmerle: performed the single-fibre EMG in both patients; Werner Stenzel: did the neuropathological investigations, provided material and antibodies; Markus Schuelke: phenotyped and treated the patients, did the clinical and neurophysiological investigations, performed WES, did the bioinformatic analysis of the genetic data, provided funding, supervised the research; Jana Marie Schwarz: supervised the research, provided funding, wrote the first draft of the manuscript together with CYL. All authors read the manuscript for intellectual content and gave consent for publishing.

Data availability statement

The data that supports the findings of this study are available in the Supporting Information of this article and are available from the corresponding author upon reasonable request. The genomic data are not publicly available due to privacy or ethical restrictions.

References

- Rodríguez Cruz PM, Palace J, Beeson D. The neuromuscular junction and wide heterogeneity of congenital myasthenic syndromes. *Int J Mol Sci* 2018; **19**: 1677. <https://doi.org/10.3390/ijms19061677>
- Engel AG, Shen X-M, Selcen D, Sine SM. Congenital myasthenic syndromes: pathogenesis, diagnosis, and treatment. *Lancet Neurol* 2015; **14**: 420–34. [https://doi.org/10.1016/S1474-4422\(14\)70201-7](https://doi.org/10.1016/S1474-4422(14)70201-7)
- Sakamoto I, Kishida S, Fukui A, Kishida M, Yamamoto H, Hino S, et al. A novel β -catenin-binding protein inhibits β -catenin-dependent Tcf activation and axis formation. *J Biol Chem* 2000; **275**: 32871–8. <https://doi.org/10.1074/jbc.M004089200>
- Kunkel GR, Tracy JA, Jalufka FL, Lekven AC. CHD8short, a naturally-occurring truncated form of a chromatin remodeler lacking the helicase domain, is a potent transcriptional coregulator. *Gene* 2018; **641**: 303–309. <https://doi.org/10.1016/j.gene.2017.10.058>
- Thompson BA, Tremblay V, Lin G, Bochar DA. CHD8 is an ATP-dependent chromatin remodeling factor that regulates β -catenin target genes. *Mol Cell Biol* 2008; **28**: 3894–904. <https://doi.org/10.1128/MCB.00322-08>
- Kobayashi M, Kishida S, Fukui A, Michiue T, Miyamoto Y, Okamoto T, et al. Nuclear localization of Duplin, a β -catenin-binding protein, is essential for its inhibitory activity on the WNT signaling pathway. *J Biol Chem* 2002; **277**: 5816–22. <https://doi.org/10.1074/jbc.M108433200>
- Nishiyama M, Skoultchi AI, Nakayama KI. Histone H1 recruitment by CHD8 is essential for suppression of the WNT- β -catenin signaling pathway. *Mol Cell Biol* 2012; **32**: 501–12. <https://doi.org/10.1128/MCB.06409-11>
- Willert K, Nusse R. WNT proteins. *Cold Spring Harb Perspect Biol* 2012; **4**: a007864. <https://doi.org/10.1101/cshperspect.a007864>
- Logan CY, Nusse R. The WNT signaling pathway in development and disease. *Annu Rev Cell Dev Biol* 2004; **20**: 781–810. <https://doi.org/10.1146/annurev.cellbio.20.010403.113126>
- Wang J, Ruan N-J, Qian L, Lei W, Chen F, Luo Z-G. WNT/ β -catenin signaling suppresses rapsyn expression and inhibits acetylcholine receptor clustering at the neuromuscular junction. *J Biol Chem* 2008; **283**: 21668–75. <https://doi.org/10.1074/jbc.M709939200>
- Koles K, Budnik V. WNT signaling in neuromuscular junction development. *Cold Spring Harb Perspect Biol* 2012; **4**: a008045. <https://doi.org/10.1101/cshperspect.a008045>
- Yan M, Li G, An J. Discovery of small molecule inhibitors of the WNT/ β -catenin signaling pathway by targeting β -catenin/Tcf4 interactions. *Exp Biol Med* 2017; **242**: 1185–97. <https://doi.org/10.1177/1535370217708198>
- Subtil-Rodríguez A, Vázquez-Chávez E, Ceballos-Chávez M, Rodríguez-Paredes M, Martín-Subero JI, Esteller M, et al. The chromatin remodeler CHD8 is required for E2F-dependent transcription activation of S-phase genes. *Nucleic Acids Res* 2014; **42**: 2185–96. <https://doi.org/10.1093/nar/gkt1161>
- Durak O, Gao F, Kaeser-Woo YJ, Rueda R, Martorell AJ, Nott A, et al. Chd8 mediates cortical neurogenesis via transcriptional regulation of cell cycle and WNT signaling. *Nat Neurosci* 2016; **19**: 1477–88. <https://doi.org/10.1038/nn.4400>
- Landon-Cardinal O, Devilliers H, Chavarot N, Mariampillai K, Rigolet A, Hervier B, et al. Responsiveness to change of 5-point MRC scale, endurance and functional evaluation for assessing myositis in daily clinical practice. *J Neuromuscul Dis* 2019; **6**: 99–107. <https://doi.org/10.3233/JND-180358>
- Li H, Durbin R. Fast and accurate long-read alignment with Burrows-Wheeler transform. *Bioinformatics* 2010; **26**: 589–95. <https://doi.org/10.1093/bioinformatics/btp698>
- McKenna A, Hanna M, Banks E, Sivachenko A, Cibulskis K, Kernysky A, et al. The genome analysis toolkit: a MapReduce framework for analyzing next-generation DNA sequencing data. *Genome Res* 2010; **20**: 1297–303. <https://doi.org/10.1101/gr.107524.110>
- Schwarz JM, Cooper DN, Schuelke M, Seelow D. MutationTaster2: mutation prediction for the deep-sequencing age. *Nat Methods* 2014; **11**: 361–2. <https://doi.org/10.1038/nmeth.2890>
- Petkova MV, Morales-Gonzales S, Relizani K, Gill E, Seifert F, Radke J, et al. Characterization of a DmdEGFP reporter mouse as a tool to investigate dystrophin expression. *Skelet Muscle* 2016; **6**: 25. <https://doi.org/10.1186/s13395-016-0095-5>
- Pasut A, Jones AE, Rudnicki MA. Isolation and culture of individual myofibers and their satellite cells from adult skeletal muscle. *J Vis Exp* 2013; **73**. <https://doi.org/10.3791/50074>
- Schneider CA, Rasband WS, Eliceiri KW. NIH image to ImageJ: 25 years of image analysis. *Nat Methods* 2012; **9**: 671–75
- Richards S, Aziz N, Bale S, Bick D, Das S, Gastier-Foster J, et al. Standards and guidelines for the

- interpretation of sequence variants: a joint consensus recommendation of the American College of Medical Genetics and Genomics and the Association for Molecular Pathology. *Genet Med* 2015; **17**: 405–23. <https://doi.org/10.1038/gim.2015.30>
- 23 Breuss MW, Gleeson JG. When size matters: CHD8 in autism. *Nat Neurosci* 2016; **19**: 1430–2. <https://doi.org/10.1038/nn.4431>
 - 24 Katayama Y, Nishiyama M, Shoji H, Ohkawa Y, Kawamura A, Sato T, et al. CHD8 haploinsufficiency results in autistic-like phenotypes in mice. *Nature* 2016; **537**: 675–9. <https://doi.org/10.1038/nature19357>
 - 25 Zahir F, Firth HV, Baross A, Delaney AD, Eydoux P, Gibson WT, et al. Novel deletions of 14q11.2 associated with developmental delay, cognitive impairment and similar minor anomalies in three children. *J Med Genet* 2007; **44**: 556–61. <https://doi.org/10.1136/jmg.2007.050823>
 - 26 Iossifov I, Ronemus M, Levy D, Wang Z, Hakker I, Rosenbaum J, et al. De novo gene disruptions in children on the autistic spectrum. *Neuron* 2012; **74**: 285–99. <https://doi.org/10.1016/j.neuron.2012.04.009>
 - 27 Neale BM, Kou Y, Liu L, Ma'ayan A, Samocha KE, Sabo A, et al. Patterns and rates of exonic de novo mutations in autism spectrum disorders. *Nature* 2012; **485**: 242–5. <https://doi.org/10.1038/nature11011>
 - 28 Talkowski ME, Rosenfeld JA, Blumenthal I, Pillalamarri V, Chiang C, Heilbut A, et al. Sequencing chromosomal abnormalities reveals neurodevelopmental loci that confer risk across diagnostic boundaries. *Cell* 2012; **149**: 525–37. <https://doi.org/10.1016/j.cell.2012.03.028>
 - 29 Bernier R, Golzio C, Xiong B, Stessman HA, Coe BP, Penn O, et al. Disruptive CHD8 mutations define a subtype of autism early in development. *Cell* 2014; **158**: 263–76. <https://doi.org/10.1016/j.cell.2014.06.017>
 - 30 De Rubeis S, He X, Goldberg AP, Poultney CS, Samocha K, Ercument Cicek A, et al. Synaptic, transcriptional and chromatin genes disrupted in autism. *Nature* 2014; **515**: 209–15. <https://doi.org/10.1038/nature13772>
 - 31 McCarthy SE, Gillis J, Kramer M, Lihm J, Yoon S, Bernstein Y, et al. De novo mutations in schizophrenia implicate chromatin remodeling and support a genetic overlap with autism and intellectual disability. *Mol Psychiatry* 2014; **19**: 652–8. <https://doi.org/10.1038/mp.2014.29>
 - 32 O'Roak BJ, Stessman HA, Boyle EA, Witherspoon KT, Martin B, Lee C, et al. Recurrent de novo mutations implicate novel genes underlying simplex autism risk. *Nat Commun* 2014; **5**: 5595. <https://doi.org/10.1038/ncomms6595>
 - 33 Prontera P, Ottaviani V, Toccaceli D, Rogaia D, Ardisia C, Romani R, et al. Recurrent 100 Kb microdeletion in the chromosomal region 14q11.2, involving CHD8 gene, is associated with autism and macrocephaly. *Am J Med Genet A* 2014; **164**: 3137–41. <https://doi.org/10.1002/ajmg.a.36741>
 - 34 Drabova J, Seemanova E, Hancarova M, Pourova R, Horacek M, Jancuskova T, et al. Long term follow-up in a patient with a de novo microdeletion of 14q11.2 involving CHD8. *Am J Med Genet A* 2015; **167**: 837–41. <https://doi.org/10.1002/ajmg.a.36957>
 - 35 Merner N, d'Arc BF, Bell SC, MauSSION G, Peng H, Gauthier J, et al. A de novo frameshift mutation in chromodomain helicase DNA-binding domain 8 (CHD8): a case report and literature review. *Am J Med Genet A* 2016; **170**: 1225–35. <https://doi.org/10.1002/ajmg.a.37566>
 - 36 Stolerman ES, Smith B, Chaubey A, Jones JR. CHD8 intragenic deletion associated with autism spectrum disorder. *Eur J Med Genet* 2016; **59**: 189–94. <https://doi.org/10.1016/j.ejmg.2016.02.010>
 - 37 Stessman HAF, Xiong B, Coe BP, Wang T, Hoekzema K, Fenckova M, et al. Targeted sequencing identifies 91 neurodevelopmental-disorder risk genes with autism and developmental-disability biases. *Nat Genet* 2017; **49**: 515–26. <https://doi.org/10.1038/ng.3792>
 - 38 Douzgou S, Liang HW, Metcalfe K, Somarathi S, Tischkowitz M, Mohamed W, et al. The clinical presentation caused by truncating CHD8 variants. *Clin Genet* 2019. <https://doi.org/10.1111/cge.13554>
 - 39 Ostrowski PJ, Zachariou A, Loveday C, Beleza B, Meireles A, Bertoli M, Dean J, et al. The CHD8 overgrowth syndrome: A detailed evaluation of an emerging overgrowth phenotype in 27 patients. *Am J Med Genet C Semin Med Genet*. <https://doi.org/10.1002/ajmg.c.31749>
 - 40 Siepel A, Bejerano G, Pedersen JS, Hinrichs AS, Hou M, Rosenbloom K, et al. Evolutionarily conserved elements in vertebrate, insect, worm, and yeast genomes. *Genome Res* 2005; **15**: 1034–50. <https://doi.org/10.1101/gr.3715005>
 - 41 Pollard KS, Hubisz MJ, Rosenbloom KR, Siepel A. Detection of nonneutral substitution rates on mammalian phylogenies. *Genome Res* 2010; **20**: 110–21. <https://doi.org/10.1101/gr.097857.109>
 - 42 Grantham R. Amino acid difference formula to help explain protein evolution. *Science* 1974; **185**: 862–4. <https://doi.org/10.1126/science.185.4154.862>
 - 43 Wu H, Xiong WC, Mei L. To build a synapse: signaling pathways in neuromuscular junction assembly. *Dev Camb Engl* 2010; **137**: 1017–33. <https://doi.org/10.1242/dev.038711>
 - 44 Takamori M. Synaptic homeostasis and its immunological disturbance in neuromuscular junction disorders. *Int J Mol Sci* 2017; **18**: 896. <https://doi.org/10.3390/ijms18040896>
 - 45 Gordon LR, Gribble KD, Syrett CM, Granato M. Initiation of synapse formation by WNT-induced MuSK

- endocytosis. *Development* 2012; **139**: 1023–33. <https://doi.org/10.1242/dev.071555>
- 46 Barik A, Lu Y, Sathyamurthy A, Bowman A, Shen C, Li L, et al. LRP4 is critical for neuromuscular junction maintenance. *J Neurosci* 2014; **34**: 13892–905. <https://doi.org/10.1523/JNEUROSCI.1733-14.2014>
- 47 Ohkawara B, Cabrera-Serrano M, Nakata T, Milone M, Asai N, Ito K, et al. LRP4 third beta-propeller domain mutations cause novel congenital myasthenia by compromising agrin-mediated MuSK signaling in a position-specific manner. *Hum Mol Genet* 2014; **23**: 1856–68. <https://doi.org/10.1093/hmg/ddt578>
- 48 DeChiara TM, Bowen DC, Valenzuela DM, Simmons MV, Poueymirou WT, Thomas S, et al. The receptor tyrosine kinase MuSK is required for neuromuscular junction formation in vivo. *Cell* 1996; **85**: 501–12. [https://doi.org/10.1016/s0092-8674\(00\)81251-9](https://doi.org/10.1016/s0092-8674(00)81251-9)
- 49 Gautam M, Noakes PG, Moscoso L, Rupp F, Scheller RH, Merlie JP, et al. Defective neuromuscular synaptogenesis in agrin-deficient mutant mice. *Cell* 1996; **85**: 525–35. [https://doi.org/10.1016/s0092-8674\(00\)81253-2](https://doi.org/10.1016/s0092-8674(00)81253-2)
- 50 Kim N, Stiegler AL, Cameron TO, Hallock PT, Gomez AM, Huang JH, et al. Lrp4 is a receptor for Agrin and forms a complex with MuSK. *Cell* 2008; **135**: 334–42. <https://doi.org/10.1016/j.cell.2008.10.002>
- 51 Zhang B, Luo S, Wang Q, Suzuki T, Xiong WC, Mei L. LRP4 serves as a coreceptor of agrin. *Neuron* 2008; **60**: 285–297. <https://doi.org/10.1016/j.neuron.2008.10.006>
- 52 Gautam M, Noakes PG, Mudd J, Nichol M, Chu GC, Sanes JR, et al. Failure of postsynaptic specialization to develop at neuromuscular junctions of rapsyn-deficient mice. *Nature* 1995; **377**: 232–6. <https://doi.org/10.1038/377232a0>
- 53 Zhang B, Luo S, Dong X-P, Zhang X, Liu C, Luo Z, et al. Beta-catenin regulates acetylcholine receptor clustering in muscle cells through interaction with rapsyn. *J Neurosci* 2007; **27**: 3968–73. <https://doi.org/10.1523/JNEUROSCI.4691-06.2007>
- 54 Luo S, Zhang B, Dong X-P, Tao Y, Ting A, Zhou Z, et al. HSP90 β regulates rapsyn turnover and subsequent AChR cluster formation and maintenance. *Neuron* 2008; **60**: 97–110. <https://doi.org/10.1016/j.neuron.2008.08.013>
- 55 Uhlén M, Fagerberg L, Hallström BM, Lindskog C, Oksvold P, Mardinoglu A, et al. Tissue-based map of the human proteome. *Science* 2015; **347**: 1260419. <https://doi.org/10.1126/science.1260419>
- 56 Platt RJ, Zhou Y, Slaymaker IM, Shetty AS, Weisbach NR, Kim J-A, et al. Chd8 mutation leads to autistic-like behaviors and impaired striatal circuits. *Cell Rep* 2017; **19**: 335–50. <https://doi.org/10.1016/j.celrep.2017.03.052>
- 57 Wilkinson B, Grepo N, Thompson BL, Kim J, Wang K, Evgrafov OV, et al. The autism-associated gene chromodomain helicase DNA-binding protein 8 (CHD8) regulates noncoding RNAs and autism-related genes. *Transl Psychiatry* 2015; **5**: e568. <https://doi.org/10.1038/tp.2015.62>
- 58 Chakkalakal JV, Jasmin BJ. Localizing synaptic mRNAs at the neuromuscular junction: it takes more than transcription. *BioEssays* 2003; **25**: 25–31. <https://doi.org/10.1002/bies.10205>
- 59 Martinou JC, Falls DL, Fischbach GD, Merlie JP. Acetylcholine receptor-inducing activity stimulates expression of the epsilon-subunit gene of the muscle acetylcholine receptor. *Proc Natl Acad Sci U S A* 1991; **88**: 7669–73. <https://doi.org/10.1073/pnas.88.17.7669>
- 60 Sandrock AW, Dryer SE, Rosen KM, Gozani SN, Kramer R, Theill LE, et al. Maintenance of acetylcholine receptor number by neuregulins at the neuromuscular junction in vivo. *Science* 1997; **276**: 599–603. <https://doi.org/10.1126/science.276.5312.599>
- 61 Li X-M, Dong X-P, Luo S-W, Zhang B, Lee D-H, Ting AKL, et al. Retrograde regulation of motoneuron differentiation by muscle β -catenin. *Nat Neurosci* 2008; **11**: 262–8. <https://doi.org/10.1038/nn2053>
- 62 Moransard M, Borges LS, Willmann R, Marangi PA, Brenner HR, Ferns MJ, et al. Agrin regulates rapsyn interaction with surface acetylcholine receptors, and this underlies cytoskeletal anchoring and clustering. *J Biol Chem* 2003; **278**: 7350–9. <https://doi.org/10.1074/jbc.M210865200>

Supporting information

Additional Supporting Information may be found in the online version of this article at the publisher's web-site:

Figure S1. Jitter histograms of the single-fibre EMG recordings.

Figure S2. CHD8/golgin co-immunostaining of patient and control fibroblasts showing a diffuse cytoplasmic distribution of CHD8 with clear enrichment around the Golgi apparatus with no difference in subcellular distribution of CHD8 between patients and controls. The white boxes in the overlay are depicted at higher magnification at the far right.

Figure S3. CHD8/rapsyn co-immunostaining of deltoid muscle sections showing neuromuscular endplates with adjacent localization of CHD8/Duplin and rapsyn at different resolutions.

Figure S4. Maximum intensity z-projection of SIM images depicted on Figure 3.

Figure S5. Separation of rendered single-SIM channels of Figure 3.

Table S1. Overview about clinical symptoms of the here reported patients and of three further individuals with heterozygous *CHD8* missense mutations or deletions of one amino acid, who have been published to date.

Table S2. Variants that cause an amino acid exchange were predicted to be potentially disease causing by the MutationTaster2 software, and have a low allele frequency in the 1000 G and gnomAD databases.

Video S1. Rotation and zoom of the volume element recorded by structured illumination microscopy from

the neuromuscular junction of a single-mouse muscle fibre.

Video S2. Rotation and zoom of the volume element recorded by structured illumination microscopy from the neuromuscular junction of a single-mouse muscle fibre.

Received 9 May 2019

Accepted after revision 23 March 2020

Published online Article Accepted on 8 April 2020